

行政院國家科學委員會專題研究計畫 成果報告

黴菌毒素 Patulin 誘發之訊號傳遞對細胞毒性的影響(2/2)

計畫類別：個別型計畫

計畫編號：NSC94-2313-B-040-001-

執行期間：94年08月01日至95年07月31日

執行單位：中山醫學大學生物醫學科學學系

計畫主持人：劉秉慧

計畫參與人員：吳亭萱

報告類型：完整報告

處理方式：本計畫可公開查詢

中 華 民 國 95 年 10 月 31 日

行政院國家科學委員會補助專題研究計畫 成果報告

計畫名稱

黴菌毒素 Patulin 誘發之訊號傳遞對細胞毒性的影響

計畫類別： 個別型計畫 整合型計畫

計畫編號：NSC — — — — —

執行期間：93 年 8 月 1 日至 95 年 7 月 31 日

計畫主持人：劉秉慧

共同主持人：

計畫參與人員：吳亭萱

成果報告類型(依經費核定清單規定繳交)： 精簡報告 完整報告

本成果報告包括以下應繳交之附件：

- 赴國外出差或研習心得報告一份
- 赴大陸地區出差或研習心得報告一份
- 出席國際學術會議心得報告及發表之論文各一份
- 國際合作研究計畫國外研究報告書一份

處理方式：除產學合作研究計畫、提升產業技術及人才培育研究計畫、列管計畫及下列情形者外，得立即公開查詢

涉及專利或其他智慧財產權， 一年 二年後可公開查詢

執行單位：中山醫學大學生物醫學科學學系

中 華 民 國 95 年 10 月 12 日

中文摘要

棒曲毒素(Patulin, 簡稱PAT)是一種在發霉水果和其再製品中常被偵測到的黴菌毒素，主要由*Penicillium* 和 *Aspergillus*菌屬所生成。當人類胚胎腎細胞(HEK293)暴露在PAT中，會隨著劑量及時間來增強兩個主要mitogen-activated protein kinases (MAPKs)途徑的磷酸化, 包含了p38 kinase 和c-Jun N-terminal kinase (JNK)。而MAPK kinase 4 (MKK4)、c-Jun 和ATF-2的磷酸化型式也可以在PAT處理的細胞株中表現。由PAT所引發的細胞死亡會被p38抑制劑(SB203580)顯著的還原，但JNK抑制劑SP600125卻沒有相同的現象。此外不論是p38抑制劑或JNK抑制劑都與PAT所引發的DNA損傷情形沒有相關性。在PAT處理的細胞中，利用adenine使PKR不活化，會顯著的抑制JNK和ERK的磷酸化反應。若是用PAT-cysteine的共價物(PAT的化學衍生物)來處理HEK293細胞，對於MAPK訊息傳導途徑、細胞存活率以及DNA完整性並沒有顯著影響。我們的實驗結果PAT在HEK293細胞中會快速活化p38 kinase及JNK途徑，但只有p38 kinase訊息傳導途徑在PAT所誘導的細胞死亡中是有貢獻的。另外，PKR在PAT所誘發的訊息傳導途徑中扮演了重要的角色。

ABSTRACT

Patulin (PAT), a mycotoxin mainly produced by *Penicillium* and *Aspergillus*, is frequently detected in moldy fruits and fruit products. Exposure of human embryonic kidney (HEK293) cells to PAT led to a dose- and time-dependent increase in the phosphorylation of two major mitogen-activated protein kinases (MAPKs), p38 kinase and c-Jun N-terminal kinase (JNK). The phosphorylated forms of MAPK kinase 4 (MKK4), c-Jun, and ATF-2 were also seen in PAT-treated cultures. The cell death caused by PAT was significantly reduced by the p38 kinase inhibitor, SB203580, but not by the JNK inhibitor, SP600125. Neither p38 kinase nor JNK played a role in the PAT-induced DNA damage. In PAT-treated cells, inactivation of double-stranded RNA-activated protein kinase R (PKR) by the inhibitor, adenine, markedly suppressed JNK and ERK phosphorylation. Treatment of HEK293 cells with PAT-cysteine adduct, a chemical derivative of PAT, showed no effect on MAPK signaling pathways, cell viability, or DNA integrity. These results indicate that PAT causes rapid activation of p38 kinase and JNK in HEK293 cells, but only the p38 kinase signaling pathway contributes to the PAT-induced cell death. PKR also plays a role in PAT-mediated MAPK activation.

Key words: patulin, p38 kinase/JNK, cell death, PKR, human embryonic kidney cells

INTRODUCTION

Patulin (PAT), 4-hydroxy-4H-furo(3,2c)pyran-2(6H)-one (Fig. 1), is a mycotoxin frequently found in apples and apple-based products (Martins *et al.*, 2002; Tangni *et al.*, 2003). The World Health Organization (WHO) and several countries have established a safety level of 50 µg/l of PAT in apple juice. Many other foods, including grains, vegetables, pears, and peaches, have also been shown to contain PAT (CAST, 2003). PAT is reported to be a mutagen, carcinogen, and teratogen in certain experimental animals (Osswald *et al.*, 1978; Smith *et al.*, 1993); the kidney and liver are the major organs affected (Imaida *et al.*, 1982; Speijer *et al.*, 1988). Treatment of cells with PAT inhibits RNA and protein synthesis and also interferes with the activity of several enzymes (Arafat *et al.*, 1985; Hatey and Moule, 1979). PAT is an electrophilic molecule and exerts its cytotoxicity by covalently binding to essential sulfhydryl groups in proteins and amino acids (Barhoumi and Burghardt, 1996). Adducts of PAT and sulfhydryl compounds have lower toxicities than PAT (Lindroth and von Wright, 1990). However, little information is available about the specific mechanisms or molecular basis of PAT toxicity for human cells.

Many extracellular stimuli are converted into specific cellular responses through the activation of three major mitogen-activated protein kinase (MAPK) signaling pathways involving extracellular signal-regulated kinase (ERK), p38 kinase, or c-Jun N-terminal kinase (JNK). MAPKs are evolutionarily conserved serine/threonine kinases and can be activated by dual phosphorylation of tyrosine and threonine residues within their catalytic domains through various protein kinase cascades (Chang and Karin, 2001). Gene-targeting studies have shown that the physiological roles of MAPKs in mice include T cell activation and differentiation, apoptosis regulation, organogenesis, and angiogenesis (Kuida and Boucher, 2004; Nishina *et al.*, 2004). In terms of environmental stimuli, the ERK pathway is predominantly activated by mitogens, whereas p38 kinase and JNK are preferentially activated by stresses, such as ultraviolet radiation, heat, osmotic shock, and chemical mutagens (Johnson and Lapadat, 2002; Zarubin and Han, 2005). JNK and p38 kinase activity in response to stress is associated with cell cycle progression, cell death, inflammation, genome instability, and oxidative stress (Abdelmegeed *et al.*, 2004; Chao and Yang, 2001; Davis, 2000; Zarubin and Han, 2005;). However, which of these multiple roles of p38 kinase and JNK is involved at any one time is primarily dependent on the stimulus, cell type, specific isoform, and the duration and strength of kinase activity.

We have previously shown that PAT activates the ERK signaling pathway in a cell line derived from human embryonic kidney (HEK293) cells and in human peripheral blood monocytes. Phosphorylation of ERK is a major factor contributing to PAT-induced genotoxicity (Wu *et al.*, 2005). In the present study, we demonstrated that treatment of HEK293 cells with PAT led to phosphorylation of p38 kinase and JNK, but only p38 kinase activation was associated with the cytotoxicity caused by PAT. In addition, we also evaluated the effect of a PAT-cysteine adduct on the MAPK signaling process and the role of double-stranded RNA-activated protein kinase R (PKR) in PAT-activated MAPK pathways.

MATERIALS AND METHODS

Reagents. Cell culture medium and serum were obtained from Life Technologies (Grand Island, NY). Rabbit polyclonal antibodies against phospho-ERK1/2 (Thr202/Tyr204), ERK1/2, phospho-p38 (Thr180/Tyr182), p38, phospho-SAPK/JNK (Thr183/Tyr185), SAPK/JNK, phospho-MKK4 (Thr261), phospho-c-Jun (Ser63), and phospho-ATF-2 (Thr71) were purchased from Cell Signaling (Beverly, MA). SB203580 [4-(4-fluorophenyl)-2-(4-methylsulfinylphenyl)-5-(4-pyridyl)imidazole] was purchased from LC laboratories (Woburn, MA) and SP600125 [anthra(1,9-*cd*)pyrazol-6(2*H*)-one] was purchased from Calbiochem (La Jolla, CA). Horseradish peroxidase-conjugated goat anti-rabbit IgG secondary antibodies were obtained from Pierce (Rockford, IL). PAT (Fig. 1) and all other reagents were purchased from Sigma Chemical Co. (St. Louis, MO). PAT was dissolved at a concentration of 10 mM in 15% ethanol and stored at -20°C.

Cell cultures and reagents. HEK293 cells were obtained from the Bioresources Collection and Research Center, Hsinchu city, Taiwan and cultured in minimal Eagle's medium (MEM) supplemented with 10% horse serum, 100 U/ml of penicillin, and 0.1 mg/ml of streptomycin at 37°C in a humidified 5% CO₂ incubator. To maintain the minimal basal levels of phosphorylated MAPKs in cells, the cells were serum-starved by transferring to 1% horse serum for 18 h before all the following experiments.

Preparation and characterization of PAT-cysteine adduct. PAT-cysteine adducts were prepared as described by Lindroth and von Wright (1990). Equimolar amounts of crystalline PAT and cysteine (L-cysteine hydrochloride, anhydrous) were dissolved in 0.1 M citric acid-0.2 M disodium phosphate buffer and the pH of the reaction mixture was adjusted to 6.0 with sodium hydroxide. The reaction was allowed to continue for 30 min with continuous magnetic stirring and then stored at -20°C. The UV spectra of PAT standard and the adduct mixture were measured using a JascoV-530 UV-Vis spectrophotometer (Japan). For thin-layer chromatographic characterization, the adduct mixture, PAT standard and cysteine solution were spotted onto thin-layer plates (silica gel 60 F₂₅₄, MERCK). The plates were developed using butanol-acetic acid-water (40: 10: 50) and examined under UV light (254 and 365 nm). The cysteine residue is supposed to form a covalent bond with carbons 4 or 7 of PAT (Fig. 1) (Mahfoud et al., 2002). The concentration of PAT-cysteine adduct was expressed as an amount of reacted PAT per unit volume. The conversion rate was around 80%.

Preparation of whole cell extracts. Cells (5×10^5 on a 5 cm tissue culture plate) were cultured for 72 h in medium containing 10% horse serum, and then serum-starved by transferring to 1% serum for 18 h to maintain the minimal basal levels of phospho-p38 and phospho-JNK in cells. The serum-starved cells at 80% confluence were then exposed to various concentrations of PAT or vehicle (15% ethanol in 0.01 M phosphate buffer containing 0.15 M NaCl, pH 7.5, PBS) for the designated time. In experiments to determine the effects of protein kinase inhibitors, serum-starved cells were pretreated for 1h with SB203580 or SP600125 before addition of PAT or vehicle in the continued presence of the inhibitor. PAT- or vehicle-treated cells were rinsed with PBS, and lysed by addition of extraction buffer (PBS containing 5% glycerol, 1 mM dithiothriitol, 1 mM EDTA, pH 8.0, 0.5% Triton X-100, 0.8 μM aprotinin, 1 mM AEBSF, 20 μM

leupeptin, 40 μ M bestatin, 15 μ M pepstain A, 14 mM E-64, and 1 mM phenylmethylsulfonyl fluoride). The cell lysate was kept on ice for 10 min, and then centrifuged at 16,000 g for 20 min at 4°C. The protein concentration of the supernatant solution was determined using the Bradford protein assay (Bio-Rad, Hercules, CA) with bovine serum albumin as the standard.

Detection of MAPK phosphorylation. Equal amounts of proteins (40 μ g) from each sample preparation were incubated for 3 min at 95°C in Laemmli buffer, separated on a 10 % SDS-polyacrylamide discontinuous gel, and then electrophoretically transferred to a nitrocellulose membrane (Bio-Rad). The membrane was blocked with PBS containing 10% skimmed milk for 1 h at room temperature, then incubated for 1 h with polyclonal antibodies specific to various MAPK proteins (1: 1000 dilution), and followed by goat anti-rabbit IgG conjugated with horseradish peroxidase (1: 5000) for another 1 h. Bound antibody on the membrane was detected using an enhanced chemiluminescence detection system according to the manufacturer's manual (Amersham Pharmacia Biotech, Amersham, UK). To re-probe the membrane with another primary antibody, bound antibodies were stripped for 30 min at room temperature with RestoreTM Western Blot Stripping Buffer (Pierce, Rockford, IL) and the membrane was washed three times with PBS-Tween 20. The intensities of bands on blots were quantitated using the ImageGauge program Ver. 3.46 (Fuji Photo Film, Tokyo).

Cell viability assay. MTT reduction assay was performed according to Liu *et al.* (2003). Briefly, HEK293 cell monolayers in 96-well plates were left untreated or treated with SB203580 (10 μ M) or SP600125 (20 μ M) for 1 h and then co-incubated with various concentrations of PAT or PAT-cysteine adduct (30, 50 or 100 μ M) for 30 min. The culture medium was then replaced with 200 μ L of medium containing 0.5 mg/ml of MTT and the plates were incubated for 3 h at 37°C. The MTT-containing medium was removed again and replaced with 100 μ L of isopropanol to solubilize the converted purple dye on the culture plates. The absorbance was measured on an Optimax microplate reader (Molecular Devices, Sunnyvale, CA.) at a wavelength of 570 nm with background subtracted at 690 nm.

Single-cell gel electrophoresis (SCGE) assay. HEK293 (1×10^5 cells) were treated with 10 μ M SB203580 or 20 μ M SP600125 for 1h, and then co-incubated with vehicle alone, 7.5 or 15 μ M PAT, or 15 μ M PAT-cysteine for 1 h. The adherent cells were trypsinized, mixed with 1% low-melting-point agarose at 42°C. The mixtures were immediately transferred to CometSlides (Trevigen Inc., Gaithersburg, MD), which were then immersed for 1 h in ice-cold lysis solution (2.5 M NaCl, 100 mM EDTA pH 10, 10 mM Tris, 1% sodium lauryl sarcosinate, 1% Triton X-100, and 1% DMSO). After electrophoresis in an alkaline buffer (300 mM NaOH, 1 mM EDTA, pH 13) at 300 mA for 30 min, the DNA on the slides was stained with SYBR green I.

The image of each cell on the slide was visualized and analyzed on a fluorescence microscope (BX51, Olympus) equipped with the computer software from CometAssay III (Perceptive Instruments Ltd, UK), which calculates the tail moment value of each cell from the amount of DNA in the tail and the distance of tail migration. For each experimental point, four cultures were treated independently and DNA damage levels in 80 cells were measured from each culture.

Measurement of protein synthesis. Inhibition of protein synthesis was measured by

³H-leucine incorporation. Briefly, HEK293 cells (6×10^5 in 1ml of complete medium) were cultured in 35 mm tissue culture plates overnight, and then the medium was replaced with 1ml of Dulbecco's modified MEM lacking leucine (DMEM/-Leu, Bioresource Inc., CA). One hour after the replacement, PAT (10-30 μ M) along with 10 μ Ci of L-[3,4,5-³H(N)] leucine (NEN Life Science Products, Inc., MA) were added into the cultures and incubated for another 3 h. Monolayer cells were lysed by addition of 500 μ l of extraction buffer as previously described and kept on ice for 10 min. After centrifuged at 16,000 g for 20 min, the cell supernatant was precipitated with 125 μ l of 50% (w/v) trichloroacetic acid (TCA) on ice for 1 h. Precipitated samples were absorbed to glass microfiber filters (Whatman, UK) using a Sampling Manifold (Millipore, Bedford, MA). The filters were washed twice with cold 5% TCA and 95% ethanol. Radioactivity remaining on the filters was measured in 2 ml of scintillation cocktail (Amersham Pharmacia Biotech, UK) using TRI-CARB 2100TR liquid scintillation counter (PerkinElmer, MA).

Statistical analysis. Values are presented as the mean \pm SEM. Statistical differences between the control and treated groups were determined using Student's *t* test and were considered significant at $p < 0.05$.

RESULTS

Effect of PAT and the adduct on the p38 kinase and JNK pathways in HEK293 cells

HEK293 cells were exposed to various concentrations of PAT for different times and the whole cell protein extract were subjected to Western blotting using specific antibodies. As shown in Fig. 2A, exposure of cells to PAT for 30 min resulted in a dose-dependent increase in p38 kinase phosphorylation, with a 3.5- and 8.3-fold increase compared to solvent-treated controls at PAT concentrations of 30 and 50 μ M, respectively. Pretreatment for 1 h with SB203580, a specific inhibitor of p38 kinase (Cuenda *et al.*, 1995), resulted in a dramatic decrease in the phospho-p38 kinase levels induced by 30 min treatment with 30 μ M PAT (Fig. 2B). Similarly, treatment of HEK293 cells with PAT at concentrations of 15-50 μ M significantly elevated the levels of phospho-JNK. PAT administration also enhanced the signals of phospho-MKK4, phospho-c-Jun, and phospho-ATF-2 (Fig. 3A). MKK4 is known to be the upstream activator of JNK, while c-Jun and ATF-2 are the downstream substrates of JNK (Davis, 2000). Pretreatment of cultures with SP600125, a specific inhibitor of JNK (Bennett *et al.*, 2001), effectively reduced the increased levels of phospho-JNK, phospho-c-Jun, and phospho-ATF-2 induced by 50 μ M PAT, but not that of phospho-MKK4 (Fig. 3B). When HEK293 cells were incubated with 15 μ M PAT for various times, phospho-p38 kinase and phospho-JNK were detected within 15 min and 30 min, respectively, and remained detectable for at least 2 h (Fig. 4).

Since the adduct of PAT-sulphydryl compound has lower toxicities than PAT (Lindroth and von Wright, 1990), a PAT-cysteine adduct was prepared to investigate its ability to activate the MAPK signaling pathways. The PAT-cysteine adduct at a concentration as high as 45 μ M had no effect on phosphorylation levels of ERK, p38 kinase, and JNK in HEK293 cell cultures (data not shown), whereas 15 μ M PAT was able to activate all the examined MAPKs. Exposure to PAT did not cause an obvious change in the levels of the non-phosphorylated forms of each MAPK (Figs.

2-4), suggesting that PAT treatment increases the phosphorylation of preexisting MAPKs, rather than *de novo* protein synthesis.

Effects of MAPK inhibitors on PAT-induced DNA damage

ERK pathway activation has been shown to be involved in PAT-induced DNA damage (Wu *et al.*, 2005). To explore the involvement of other MAPKs, HEK293 cells were left untreated or treated with MAPK inhibitors for 1 h before co-exposure to PAT (7.5 and 15 μ M) or PAT-cysteine adduct (15 μ M) for another 1 h, and then subjected to SCGE assays. Compared to the untreated group, HEK293 cells treated with 15 μ M PAT showed a 4-fold increase in tail moment value (4.66 ± 0.45); this increase was not significantly affected in the presence of SB203580 or SP600125 (Table 1). Similar results were observed in 7.5 μ M PAT-treated cultures, suggesting that activation of p38 kinase and JNK does not contribute to PAT-induced DNA damage. Treatment of cells with 15 μ M PAT-cysteine adduct had no effect on the tail moment value, showing that the PAT-cysteine adduct did not cause DNA damage in HEK293 cells.

Effect of MAPK inhibitors on PAT-induced changes in cell morphology and viability

To study the relationship between the MAPK signaling and cytotoxicity induced by PAT, HEK293 cells were left untreated or were pretreated with SB203580 or SP600125 for 1 h before co-exposure to 30 μ M PAT for another 3 or 5 h, and then cell morphology and viability were examined. When HEK293 cells were exposed to PAT alone, cell shrinkage and detachment were observed under microscope (Fig. 5). SB203580 almost totally prevented the damage caused by PAT, while SP600125 had no effect. The roles of p38 kinase and JNK in PAT-induced cytotoxicity were further investigated using the MTT assay, a method using the activity of mitochondrial succinate dehydrogenase as an indicator of cell viability. As shown in Fig. 6, the viability of HEK293 cells was significantly reduced to 74.5 or 51.4 % of control levels following 30 min treatment with 50 or 100 μ M PAT, respectively, while no cytotoxicity was detected in cultures exposed to PAT-cysteine adduct even at a concentration of 100 μ M. Pretreatment with SB203580, but not SP600125, resulted in a marked decrease in cytotoxicity in PAT-treated cultures. Neither SB203580 nor SP600125 alone had a cytotoxic effect (data not shown). Thus, our data suggest that the p38 kinase pathway, but not the JNK pathway, is involved in PAT-induced cell death.

Induction of MAPK phosphorylation through PKR activation Certain xenobiotics modulate MAP kinases through a process referred to as “ribotoxic stress response” and these ribotoxic stressors at least partially inhibit protein synthesis (Laskin *et al.*, 2002). In the ribotoxic stress response, PKR, an enzyme associating with ribosomes via specific recognition sites and with translation inhibition ability, seems to function as a signal integrator for activation of MAPKs (Wu *et al.*, 1998; Zhou *et al.*, 2003). The above information prompted us to examine whether PAT caused inhibition of protein synthesis. As shown in Fig. 7, HEK293 cells treated for 3 h with 20 or 30 μ M PAT showed a reduction in H^3 -labelled leucine incorporation to approximately 57.4 or 29.6% of control levels, respectively. To evaluate the playing role of PKR in PAT-activated MAPK signaling, HEK293 cells were pretreated for 1 h with adenine, a PKR inhibitor, before co-exposure to PAT. As shown in Fig. 8, both the ERK and JNK phosphorylation induced by PAT were dramatically inhibited in the presence of adenine; a similar, but weaker, effect was seen for phosphorylated p38 kinase. Anisomycin, a compound known to cause MAPK activation through

PKR (Zhou *et al.*, 2003), was used as a positive control. Our results indicate that PKR activation may contribute to the PAT-induced activation of the ERK and JNK pathways, and, to a much lesser extent, of the p38 kinase pathway.

DISCUSSION

Surveys of samples from certain countries have revealed that the PAT content in some commercialized products exceeds the safety level (50 µg/l) established by the WHO (Lai *et al.*, 2000; Yurdun *et al.*, 2001). Although previous *in vitro* and *in vivo* studies have shown that PAT has a broad toxicity spectrum, the cellular and molecular mechanisms of PAT toxicity for human cells are still not clear. Treatment of HEK293 cells with PAT resulted in a dose- and time-dependent increase in p38 kinase and JNK phosphorylation (Figs. 2 and 3). We have previously demonstrated that treatment of human cells with PAT activates the ERK pathway (Wu *et al.*, 2005). The induction patterns of phosphorylated ERK, p38 kinase, and JNK by PAT were very similar. Treatment of cells with 15 µM PAT for 30 min was sufficient to detect the phosphorylated forms of each MAPK, implying that PAT causes a rapid induction of phosphorylation of all MAPKs without special preference and may trigger their activation through a common upstream factor.

The observed phosphorylation of MKK4 suggests that MKK4 is the upstream activator of JNK in PAT-treated cultures (Fig. 3), but we cannot rule out the involvement of MKK7. Both MKK4 and MKK7 are reported to be upstream activators of JNK by various stimuli. MKK4 is primarily activated by environmental stress and MKK7 is primarily activated by cytokines (e.g. TNF and IL-1), so these two kinases might contribute differentially to JNK activation (Davis, 2002). Phosphorylated JNK undergoes dimerization and translocates into the nucleus to phosphorylate certain transcriptional factors, including c-Jun and ATF-2; ATF-2 is also activated by p38 kinase pathway (Whitmarsh and Davis, 1996). Phosphorylation of c-Jun and ATF-2 increases their trans-acting DNA binding activity; c-Jun homodimers bind to the AP-1 consensus sequence (Halazonetis *et al.*, 1988) and c-Jun/ATF-2 heterodimers prefer the ATF/CREB consensus sequence (Benbrook and Jones, 1990). High levels of phospho-c-Jun and ATF-2 proteins correlate with tumor progression in the mouse skin carcinogenesis model (Zoumpourlis *et al.*, 2000). The above information suggests that PAT may exert its toxicity through a sequential transcriptional activation of the downstream genes modulated by c-Jun and ATF-2.

To examine the role of phospho-JNK and p38 kinase in PAT-induced toxicity, inhibitors of the individual pathways, SP600125 and SB203580, were used. SP600125 had no effect on PAT-induced changes in cell morphology and cell viability in HEK293 cell cultures (Figs. 5 and 6), suggesting that PAT-induced JNK phosphorylation is not involved in these processes. However, inhibition of p38 kinase phosphorylation by SB203580 partially prevented these changes. Since PAT treatment also led to apoptosis in HEK293 cells (data not shown), these data indicate that the p38 kinase pathway is responsible for part of the PAT-induced cell death/apoptosis. Activation of the p38 kinase may induce either cell death or cell survival in different cell types under different conditions (Anderson, 1997). Our results are in agreement with those of many previous studies, which suggested that the p38 kinase cascade is involved in

the apoptosis caused by some anti-cancer agents, heavy metals, and natural toxins (Bacus *et al.*, 2001; Smith *et al.*, 2003). On the other hand, phosphorylation of p38 kinase and JNK showed no obvious correlation with the DNA damage caused by PAT (Table 1). However, activation of ERK signaling has been shown to play a role in PAT-induced DNA damage (Wu *et al.*, 2005). It seems that each of these three MAPKs plays a different role when HEK293 cells are stimulated with PAT.

Treatment of HEK293 cells with PAT-cysteine adduct had no effect on any of the examined MAPK pathways, DNA integrity, or cell viability (Table 1 and Fig. 6), indicating that the signal-inducing ability and cytotoxicity of PAT can be completely prevented by blocking the thiol-reacting sites (C4 and C7) on the toxin with cysteine. This observation supports the hypothesis that PAT exerts its cytotoxic effects mainly by forming covalent adducts with essential cellular thiols (Mahfoud *et al.*, 2002). It is probable that PAT attacks cellular SH-containing proteins and this leads to MAPK activation.

Some chemical agents, including trichothecene mycotoxins, ultraviolet radiation, and certain protein synthesis inhibitors, work as ribotoxic stressors to interfere the function of the 3' end of the 28S rRNA, and then leads to the rapid activation of various MAPKs (Laskin *et al.*, 2002). In the process of ribotoxic stress response induced by translation inhibitors, PKR, an ubiquitously expressed serine/ threonine protein kinase activated by dsRNA, cytokines, and stress signals, plays a critical upstream role (Zhou *et al.*, 2003). In HEK293 cell cultures, PAT functioned as a translation inhibitor in a dose-dependent manner (Fig. 7). PAT has been reported to inhibit protein synthesis in the rat liver and in hepatoma tissue cultures by an unknown mechanism (Arafat and Musa, 1995; Hatey and Moule, 1979). In addition, pre-incubation of HEK293 cells with adenine, a known PKR inhibitor, abolished most of the PAT-induced phosphorylation of JNK and ERK (Fig. 8). Treatment of HEK293 cells with PAT also slightly upregulated the phosphorylation of eukaryotic translation initiation factor 2 (data not shown), a downstream substrate of PKR (Saelens *et al.*, 2001). Thus, it is highly possible that PAT triggers the JNK and ERK pathways in HEK293 cells through PKR activation.

In conclusion, our data show that PAT, a mycotoxin commonly found in apple juice and related products, activates the p38 kinase and JNK signaling pathways and their downstream transcriptional factors in human cells. Phosphorylation of p38 kinase, but not of JNK, is a major factor contributing to the cell death induced by PAT. In addition, PKR plays a role in mediating the activation of the MAPK pathways. A summarized figure is shown to describe the probable cellular mechanisms of PAT toxicity (Fig. 9). Knowledge of the adverse levels and toxicological mechanism of PAT in human cells should be useful in estimating the risk to the general public.

FIGURE LEGENDS

Fig. 1. Structure of patulin (PAT)

Fig. 2. Induction of p38 kinase phosphorylation by PAT in HEK293 cells. Subconfluent HEK293 cells were rendered quiescent by incubation for 18 h in medium containing 1% serum, and then (A) incubated for 30 min with vehicle or various PAT concentrations (5-50 μ M) or (B) pretreated for 1 h with SB203580 before co-incubation with SB20380 and 30 μ M PAT for another 30 min. Whole cell extracts were prepared immediately after treatment and p38 kinase activation was estimated by Western blotting using antibodies that recognized the phosphorylated or unphosphorylated forms of p38 kinase. The relative phospho-p38 kinase levels shown in the lower panel of (A) were densitometric analyses from two independent experiments and are expressed as the mean \pm SEM, which were normalized by arbitrarily setting the value for vehicle-treated cells as 1. * denotes a significant difference compared to the vehicle-treated group ($p < 0.05$).

Fig. 3. Phosphorylation of components of the JNK pathway in PAT-treated cells. Subconfluent HEK293 cells were rendered quiescent in medium containing 1% serum for 18 h, then (A) incubated for 30 min with vehicle or various PAT concentrations (5-50 μ M) or (B) pretreated for 1 h with SP600125 before co-incubation with SP600125 and 50 μ M PAT for another 30 min. Whole cell extracts were subjected to Western blotting using antibodies specific for phospho-JNK (Thr183/Tyr185), phospho-MKK4 (Thr261), phospho-c-Jun (Ser63), or phospho-ATF-2 (Thr71). The results are representative of those from three independent experiments.

Fig 4. Time-dependent induction of p38 kinase and JNK phosphorylation by PAT. Subconfluent HEK293 cells in medium containing 1% serum were incubated with 15 μ M PAT for up to 120 min, then whole cell extracts were prepared and subjected to Western blotting using anti-phospho-p38 kinase/JNK or anti-p38 kinase/JNK antibodies. The relative phospho-p38 kinase and phospho-JNK levels were densitometric analyses from three independent experiments and are expressed as the mean \pm SEM, which were normalized by arbitrarily setting the value for vehicle-treated cells as 1. * denotes a significant difference compared to the vehicle-treated group ($p < 0.05$).

Fig. 5. Effect of p38 kinase/JNK inhibitors on the PAT-induced cellular morphology changes. HEK293 cell cultures at 80% confluence were pre-treated with SB203580 or SP600125 (20 μ M) for 1 h, and then co-incubated with the same inhibitor plus vehicle (control group) or 30 μ M PAT for another 3 or 5 h. The images were captured with an integrating CCD camera mounted on ZEISS Axionvert 200M microscope with 100 x magnification. Phase contrast images of representative fields are shown.

Fig. 6. Effect of p38 kinase or JNK inhibitors on PAT-induced cytotoxicity. HEK293 cells were

left untreated or treated with 10 μ M SB203580 or 20 μ M SP600125 for 1 h, and then co-incubated with the same inhibitor and various concentrations of PAT or PAT-cysteine adduct (30, 50, or 100 μ M) for 30 min. Cell viability was determined using the MTT assay. The data from at least three independent experiments are expressed as the mean \pm SEM. *, significant difference ($p < 0.05$) compared to the paired group.

Fig. 7. PAT treatment reduced protein synthesis in HEK293 cells. Cells were incubated for 3 h with vehicle or various concentrations of PAT (10, 20, or 30 μ M) plus 10 μ Ci of L-[3,4,5-³H(N)] leucine. Protein synthesis was measured as described in the “Materials and Methods” and expressed as a percentage of that in cells exposed to vehicle only. The data are given as the mean \pm SEM (n=5). *, significant difference compared to the vehicle-treated group ($p < 0.05$).

Fig. 8. The PKR inhibitor, adenine, inhibited PAT-induced MAPK activation. HEK293 cultures were left untreated or were treated with 100 ng/ml of adenine for 1 h before and during exposure to PAT (50 μ M) or anisomycin (50 ng/ml) for 30 min. Cell lysates were prepared and analyzed for phosphorylated ERK, p38 kinase, and JNK by Western blotting.

Fig 9. A proposed model for PAT-induced MAPK pathways in HEK293 cells. PAT may attack cellular SH-containing proteins first and this leads to MAPK activation through the ribotoxic stress response or an unknown mechanism. ERK activation plays a role in PAT-induced DNA damage and p38 kinase activation correlates with the PAT-induced cell death.

ACKNOWLEDGMENT

This work was supported by grants NSC 92-2313-B-040-003 and 93-2313-B-040-001 from the National Science Council of the Republic of China.

REFERENCES

- Abdelmegeed, M. A., Kim, S. K., Woodcroft, K. J., and Novak, R. F. (2004). Acetoacetate activation of extracellular signal-regulated kinase 1/2 and p38 mitogen-activated protein kinase in primary cultured rat hepatocytes: role of oxidative stress. *J. Pharmacol. Exp. Ther.* **310**, 728-736.
- Anderson, P. (1997). Kinase cascades regulating entry into apoptosis. *Microbiol. Mol. Biol. Rev.* **61**, 33-46.
- Arafat, W., Kern, D., and Dirheimer, G. (1985). Inhibition of aminoacyl-tRNA synthetases by the mycotoxin patulin. *Chem. Biol. Interact.* **56**, 333-349.
- Arafat, W., and Musa, M. N. (1995). Patulin-induced inhibition of protein synthesis in hepatoma tissue culture. *Res. Commun. Mol. Pathol. Pharmacol.* **87**, 177-186.
- Bacus, S. S., Gudkov, A. V., Lowe, M., Lyass, L., Yung, Y., Komarov, A. P., Keyomarsi, K., Yarden, Y., and Seger, R. (2001). Taxol-induced apoptosis depends on MAP kinase pathways (ERK and p38) and is independent of p53. *Oncogene* **20**, 147-155.
- Barhoumi, R., and Burghardt, R. C. (1996). Kinetic analysis of the chronology of patulin- and

- gossypol-induced cytotoxicity in vitro. *Fund. Appl. Toxicol.* **30**, 290-7.
- Benbrook, D. M., and Jones, N. C. (1990). Heterodimer formation between CREB and JUN proteins. *Oncogene* **5**, 295-302.
- Bennett, B. L., Sasaki, D. T., Murray, B. W., O'Leary, E. C., Sakata, S. T., Xu, W., Leisten, J. C., Motiwala, A., Pierce, S., Satoh, Y., Bhagwat, S. S., Manning, A. M., and Anderson, D. W. (2001). SP600125, an anthrapyrazolone inhibitor of Jun N-terminal kinase. *Proc. Natl. Acad. Sci. USA* **98**, 13681-6.
- CAST. (2003). Mycotoxins: Risks in Plant, Animal, and Human Systems. Council of Agricultural Science and Technology, Task force rep. No. 139, Ames, IA.
- Chang, L., and Karin, M. (2001). Mammalian MAP kinase signalling cascades. *Nature* **410**, 37-40.
- Chao, J. I., and Yang, J. L. (2001). Opposite roles of ERK and p38 mitogen-activated protein kinases in cadmium-induced genotoxicity and mitotic arrest. *Chem. Res. Toxicol.* **14**, 1193-1202.
- Cuenda, A., Rouse, J., Doza, Y. N., Meier, R., Cohen, P., Gallagher, T. F., Young, P. R., and Lee, J. C. (1995). SB 203580 is a specific inhibitor of a MAP kinase homologue which is stimulated by cellular stresses and interleukin-1. *FEBS Letters.* **364**, 229-33.
- Davis, R. J. (2000). Signal Transduction by the JNK group of MAP kinases. *Cell* **103**, 239-252.
- Halazonetis, T. D., Georgopoulos, K., Greenberg, M. E., and Leder, P. (1988). C-Jun dimerizes with itself and with c-Fos, forming complexes of different DNA binding affinities. *Cell* **55**, 917-924.
- Hatey, F., and Moule, Y. (1979). Protein synthesis inhibition in rat liver by the mycotoxin patulin. *Toxicology* **13**, 223-231.
- Imaida, K., Hirose, M., Ogiso, T., Kurata, Y., and Ito, N. (1982). Quantitative analysis of initiating and promoting activities of five mycotoxins in liver carcinogenesis in rats. *Cancer Letters.* **16**, 137-43.
- Johnson, G. L., and Lapadat, R. (2002). Mitogen-activated protein kinase pathways mediated by ERK, JNK, and p38 protein kinases. *Science* **298**, 1911-1912.
- Kuida, K., and Boucher, D. M. (2004). Functions of MAP kinases: insights from gene-targeting studies. *J. Biochem. (Tokyo)* **135**, 653-656.
- Lai, C. L. (2000). Detection of mycotoxin patulin in apple juice. *J. Food Drug Analysis* **8**, 85-96
- Laskin, J. D., Heck, D. E., and Laskin, D. L. (2002). The ribotoxic stress response as a potential mechanism for MAP kinase activation in xenobiotic toxicity. *Toxicol. Sci.* **69**, 289-291.
- Lindroth, S., and von Wright, A. (1990) Detoxification of patulin by adduct formation with cysteine. *J. Environ. Pathol. Toxicol. Oncol.* **10**, 254-9.
- Liu, B. H., Yu, F. Y., Wu, T. S., Li, S. Y., Su, M. C., Wang, M. C., and Shih, S. M. (2003). Evaluation of genotoxic risk and oxidative DNA damage in mammalian cells exposed to mycotoxins, patulin and citrinin. *Toxicol. Appl. Pharmacol.* **191**, 255-263.
- Mahfoud, R., Maresca, M., Garmy, N., and Fantini, J. (2002). The mycotoxin patulin alters the barrier function of the intestinal epithelium: mechanism of action of the toxin and protective effects of glutathione. *Toxicol. Appl. Pharmacol.* **181**, 209-218.

- Martins, M. L., Gimeno, A., Martins, H. M., and Bernardo, F. (2002). Co-occurrence of patulin and citrinin in Portuguese apples with rotten spots. *Food Addit. Contam.* **19**, 568-74.
- Nishina, H., Wada, T., and Katada, T. (2004). Physiological roles of SAPK/JNK signaling pathway. *J. Biochem. (Tokyo)* **136**, 123-6.
- Osswald, H., Frank, H. K., Komitowski, D., and Winter, H. (1978). Long-term testing of patulin administered orally to Sprague-Dawley rats and Swiss mice. *Food Cosmet. Toxicol.* **16**, 243-7.
- Saelens, X., Kalai, M., Vandenabeele, P. (2001). Translation inhibition in apoptosis: caspase-dependent PKR activation and eIF2-alpha phosphorylation. *J. Biol. Chem.* **276**, 41620-8.
- Smith, E. E., Duffus, E. A., and Small, M. H. (1993). Effects of patulin on postimplantation rat embryos. *Arch. Environ. Contam. Toxicol.* **25**, 267-70.
- Smith, W. E., Kane, A. V., Campbell, S. T., Acheson, D. W., Cochran, B. H., and Thorpe, C. M. (2003). Shiga toxin 1 triggers a ribotoxic stress response leading to p38 and JNK activation and induction of apoptosis in intestinal epithelial cells. *Infect. Immun.* **71**, 1497-504.
- Speijers, G. J., Franken, M. A., and van Leeuwen, F. X. (1988). Subacute toxicity study of patulin in the rat: effects on the kidney and the gastro-intestinal tract. *Food Chem. Toxicol.* **26**, 23-30.
- Tangni, E. K., Theys, R., Mignolet, E., Maudoux, M., Michelet, J. Y., and Larondelle, Y. (2003). Patulin in domestic and imported apple-based drinks in Belgium: occurrence and exposure assessment. *Food Addit. Contam.* **20**, 482-9.
- Whitmarsh, A. J., and Davis, R. J. (1996). Transcription factor AP-1 regulation by mitogen-activated protein kinase signal transduction pathways. *J. Mol. Med.* **74**, 589-607.
- Wu, S. Y., Kumar, K. U., and Kaufman, R. J. (1998). Identification and requirement of three ribosome-binding domains in dsRNA-dependent protein kinase (PKR). *Biochemistry* **37**, 13816-13826.
- Wu, T. S., Yu, F. Y., Su, C. C., Kan, J. C., Chung, C. P., and Liu, B. H. (2005). Activation of ERK mitogen-activated protein kinase in human cells by the mycotoxin patulin. *Toxicol. Appl. Pharmacol.* **207**, 103-111.
- Yurdun, T., Omurtag, G. Z., and Ersoy, O. (2001). Incidence of patulin in apple juices marketed in Turkey. *J. Food Prot.* **64**, 1851-3.
- Zarubin, T., and Han, J. (2005). Activation and signaling of the p38 MAP kinase pathway. *Cell Res.* **15**, 11-8.
- Zhou, H. R., Lau, A. S., and Pestka, J. J. (2003). Role of double-stranded RNA-activated protein kinase R (PKR) in deoxynivalenol-induced ribotoxic stress response. *Toxicol. Sci.* **74**, 335-44.
- Zoumpourlis, V., Papassava, P., Linardopoulos, S., Gillespie, D., Balmain, A., and Pintzas, A. (2000). High levels of phosphorylated c-Jun, Fra-1, Fra-2 and ATF-2 proteins correlate with malignant phenotypes in the multistage mouse skin carcinogenesis model. *Oncogene* **19**, 4011-21.

Table 1. Effects of MAPK inhibitors on PAT-induced DNA damage

Treatment	Tail moment value ^a		
	–	+SB203580 (10 μ M)	+SP600125(20 μ M)
PAT (μM)			
0	1.00 \pm 0.11	0.75 \pm 0.01	1.34 \pm 0.13
7.5	2.84 \pm 0.26*	2.79 \pm 0.21*	3.40 \pm 0.19*
15.0	4.66 \pm 0.45*	4.32 \pm 0.57*	4.96 \pm 0.29*
PAT-cysteine (μM)			
15	0.84 \pm 0.31	---	---

^a HEK293 cells were left untreated or were treated with inhibitors for 1 h, then incubated with PAT or PAT-cysteine adduct for another 1 h. DNA strand breaks, expressed as tail moment values, were determined by the SCGE assay. Each data point is the mean \pm SEM from at least three independent experiments. *, significantly different when compared to cultures treated with 0 μ M PAT (p <0.05)

Fig. 1

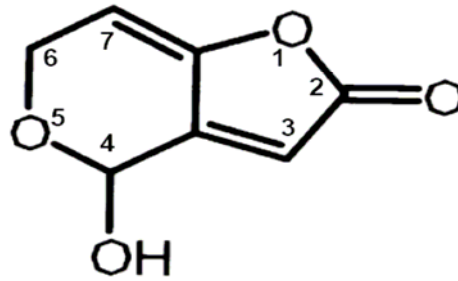


Fig. 2

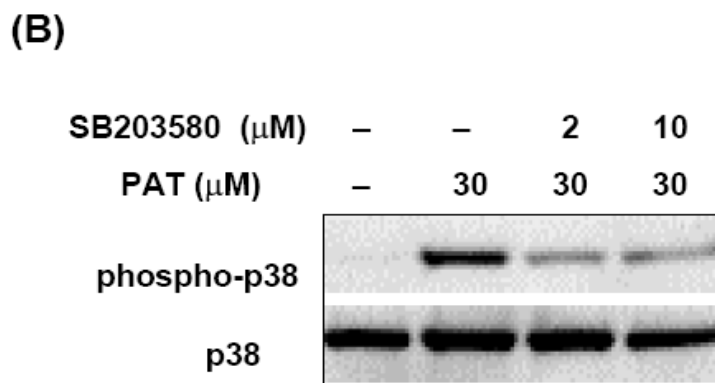
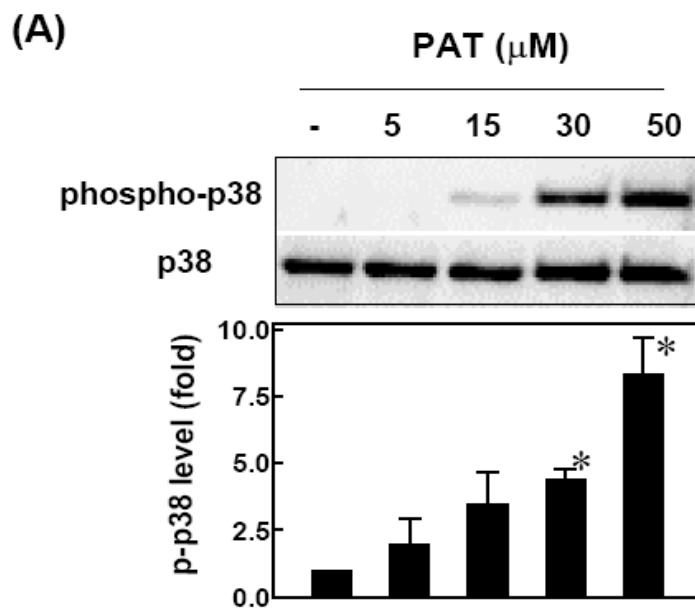


Figure 3

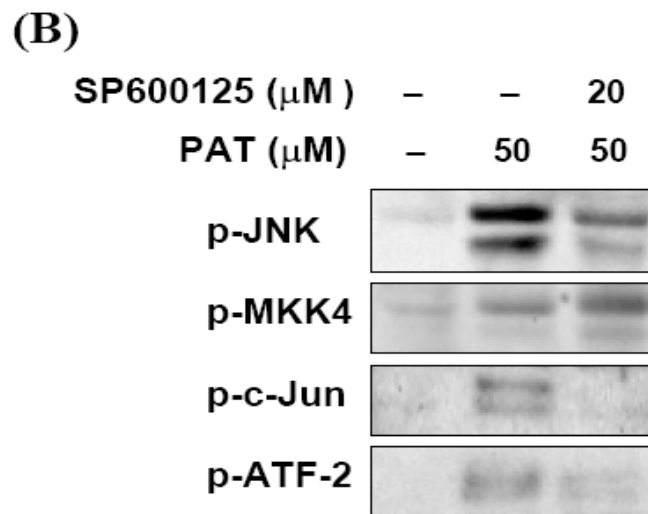
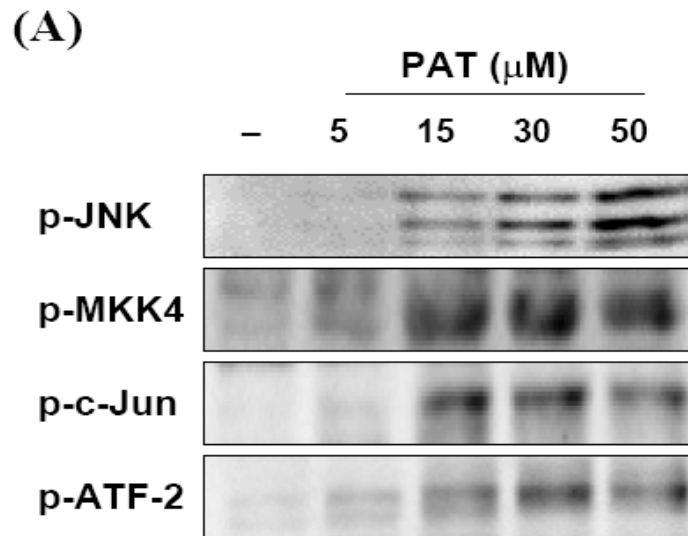


Figure 4

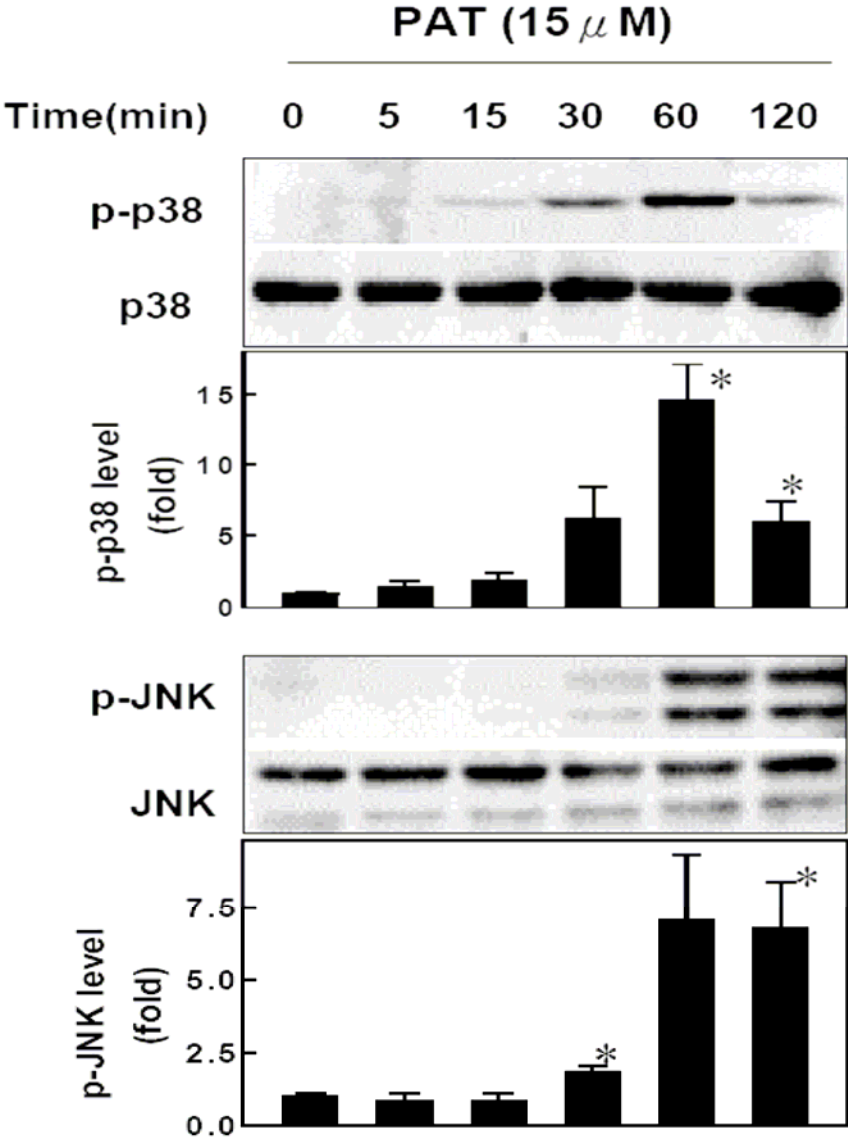


Figure 5

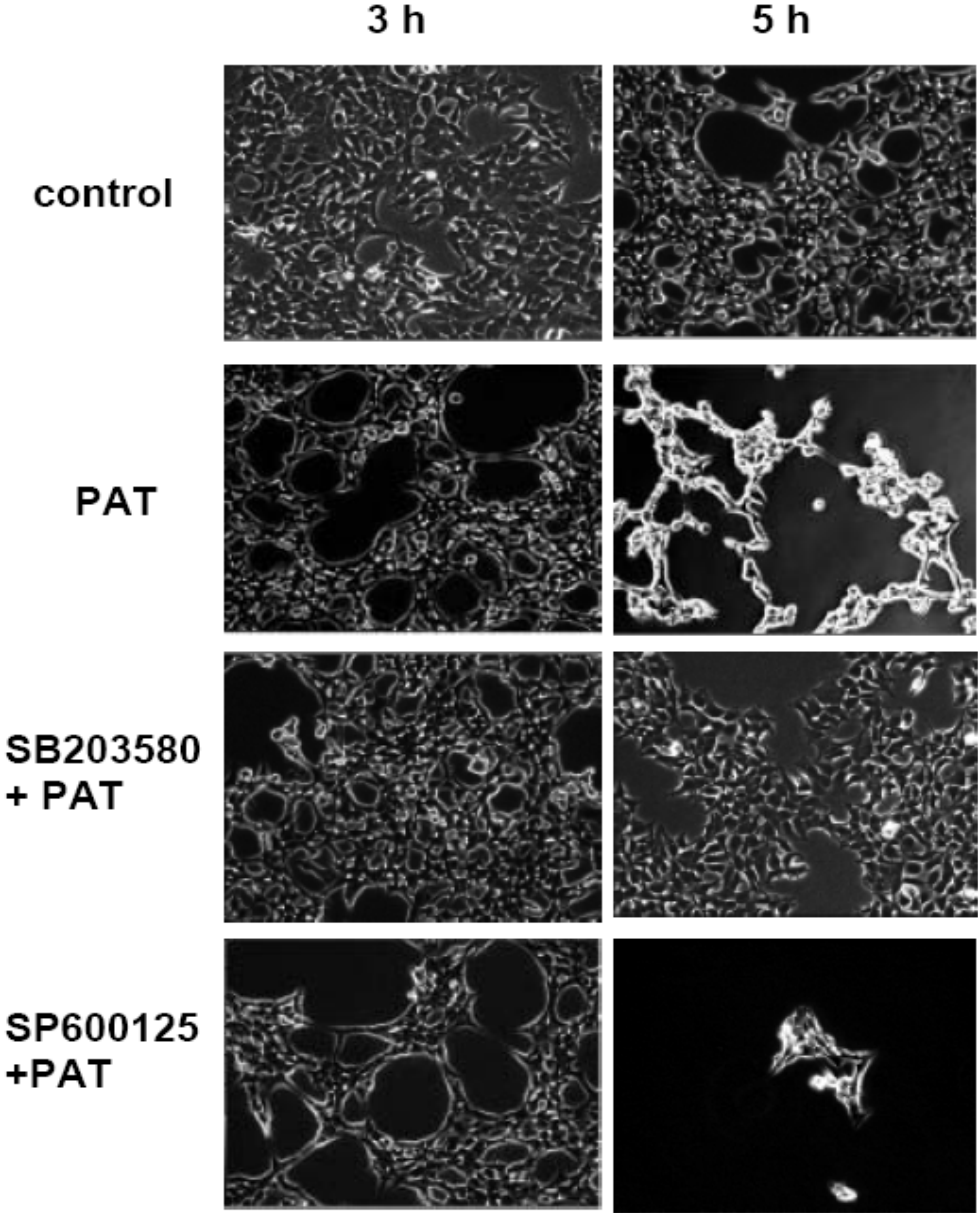


Figure 6

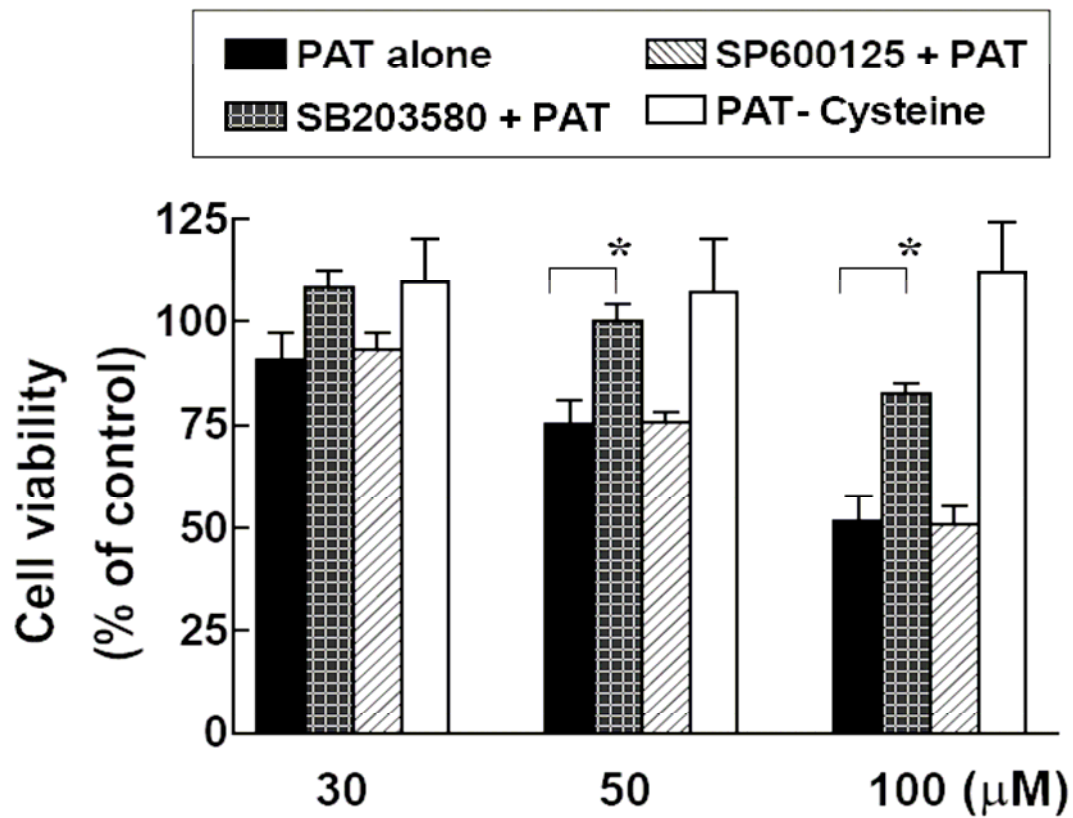


Figure 7

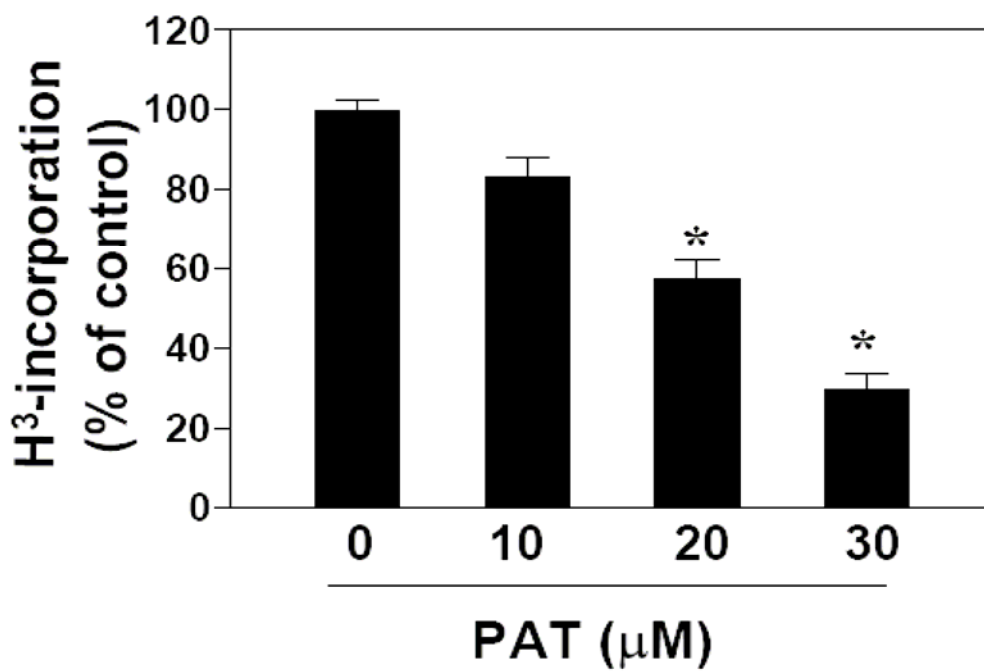


Figure 8

Anisomycin (ng/ml)	-	-	-	50	50
PAT (μ M)	-	50	50	-	-
Adenine (ng/ml)	-	-	100	-	100

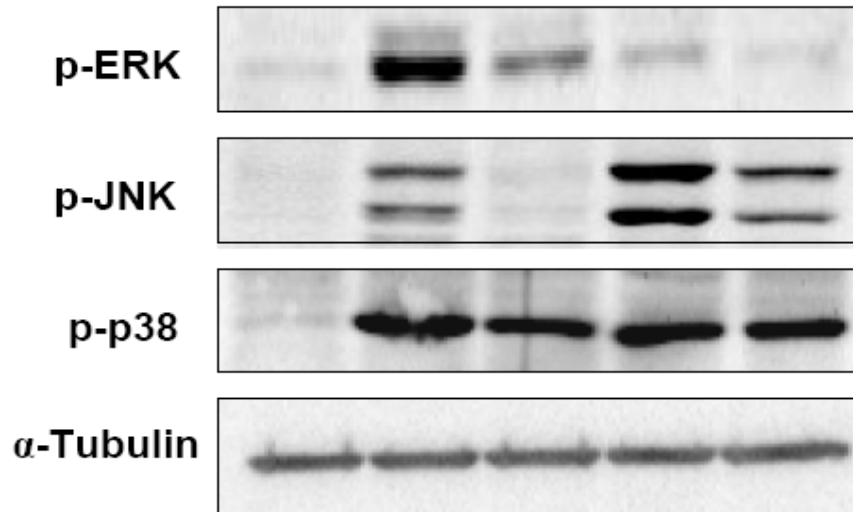


Figure 9

